Electrodeposition and characterization of nanocrystalline Fe−Ni−Cr alloy coatings synthesized via pulse current method

Ebrahim YOUSEFI[1,2], Ahmad IRANNEJAD[1,3], Shahriar SHARAFI[1,3]

1. Department of Nano technology, Mineral Industries Research Center,
Shahid Bahonar University of Kerman, Kerman 7618868366, Iran;
2. Young Researchers Society, Shahid Bahonar University of Kerman, Kerman 7618868366, Iran;
3. Department of Material Science and Engineering, Shahid Bahonar University of Kerman, Kerman 7618868366, Iran

Abstract: The nanocrystalline Fe−Ni−Cr coatings were electrodeposited by using the pulse current technique. The SEM results showed that the coatings had a mixed morphology of small nodules and fine cauliflower structures at low current densities. Also, the Cr content was increased at expense of Fe and Ni contents at high current densities. XRD patterns confirmed that the pulse current density had a positive effect on the grain refinement. The results of vibrating sample magnetometer (VSM) measurements demonstrated that by increasing the current density, the saturation magnetization was decreased and the coercivity was increased due to the enhancement of Cr content and the reduction of the grain size. The friction coefficient and wear rate values were decreased by increasing the pulse current density. Also, both the adhesive and abrasive wear mechanisms were observed on the worn surfaces. The abrasive grooves and the amount of wear debris were decreased by increasing the pulse current density.
Key words: pulse electrodeposition; current density; nanocrystalline Fe−Ni−Cr coatings; magnetic behavior; tribological properties

1 Introduction

The Fe−Ni magnetic alloys which are often called permalloys, are very important among the soft magnetic materials [1−4]. Today, Fe−Ni permalloy coatings have wide and special applications in electronic industries such as storage, recording and memory devices, magnetic heads and pole pieces in magnetic valves due to stable and unique magnetic properties [4−7]. For the mentioned electronic applications, in addition to unique magnetic properties, they should have excellent tribological properties. The Fe−Ni permalloy is a soft magnetic material with high magnetization [4−8]. However, the Fe−Ni coatings cannot meet the mentioned features due to the presence of Fe which leads to the formation of a coating with poor mechanical properties [5−9]. The presence of Cr in Fe−Ni coatings leads to the applications of these structures in the developed industries as the protective coatings for softer and more corrosive substrates [5−7,10−18].

Fe−Ni−Cr coatings can be produced by different methods, but the electrodeposition process is one of the most useful techniques for preparing these coatings with suitable chemical and mechanical properties [5−7,12−17]. Electrodeposition method can be carried out by direct current (DC), pulse current (PC) and pulse reverse current (PRC) techniques. However, the PC technique is an effective method for producing the alloy coatings with better properties compared to DC one [5−7,14]. The production of the nanocrystalline and fine-grained coatings and also the high deposition rates are the important advantages of PC electrodeposition method [6,7,9]. The peak current density (J_p), current "on" time (t_{on}), current "off" time (t_{off}), duty cycle (d) and pulse frequency (f) are the effective operational variables for the improvement of the properties of the resultant coatings. The duty cycle (d) and pulse frequency (f) are determined by Eqs. (1) and (2), respectively [7,14,19,20]:

$$d = \frac{t_{on}}{t_{on}+t_{off}} \times 100\% \tag{1}$$

$$f = \frac{1}{t_{on}+t_{off}} \tag{2}$$

The pulse current density is one of the most effective parameters in electrodeposition process because it can affect the morphology, the chemical composition and the mechanical properties of the prepared coatings [4,6−8,14]. Moreover, the electrodeposition method with pulse current density could be used to synthesize nanocrystalline alloy coatings and control thickness by regulating the pulse current density. In fact, optimizing the current density in this technique has advantages such as having higher rate of deposition, improving the adhesion of deposit, preparing finer grained coatings and also improving the magnetic and mechanical properties [6−8,19−20]. Cr-based alloy coatings can be prepared by the chloride baths containing Cr^{3+} or Cr^{6+} ions. But, the use of chloride baths with Cr^{6+} ions has been restricted due to high toxicity of the bath in the environment and carcinogenicity in humans [5,10,18]. Furthermore, today the environmental concerns caused to use Cr(III)-based baths for producing the Cr-based coatings, because the Cr(III) has fewer toxic chemical species, and thus, the use of Cr(III)-based baths has fewer risks compared to Cr(VI)-based electroplating baths [5,9−11,18]. Moreover, the low content of Cr in Fe−Ni matrix is one of the main problems in Fe−Ni−Cr coatings, and its content is usually in the range of 2−14 wt.% [6,7,9]. For simultaneous co-deposition of the Fe, Ni and Cr in aqueous solutions and increasing the Cr content in the deposits, the reduction potential of various elements should be close each other. For this purpose, two methods have been suggested as follows: (1) shifting to the static potentials of metals by changing the salt concentrations and/or using complexing materials [10,21], and (2) changing the dynamic potentials of metals by increasing the current density and/or using the additive materials [10,21]. Also, increasing the content of more active metals in the solution is one of the easiest methods [7,12,21]. Moreover, simultaneous use of sodium citrate and glycolic acid as complexing materials is an effective method for modifying the complexes of chromium [10,13,18]. Due to the low pH of chloride baths, the residual stress can build up inside the prepared coatings during the electrodeposition process and also the Fe and Cr hydroxide compounds can be produced [6,10,21,22]. Therefore, boric acid should be used as an effective buffering agent on the life of electroplating bath both by keeping pH constant at the desired levels and by preventing the formation of Fe and Cr hydroxides [6,10,21]. During Cr co-deposition, hydrogen evolution reaction happens. This behavior leads to hydrogen bubbles evolution and therefore the formation of cracks on the surface [5,7,10,22]. Therefore, careful choice of complexing materials and operating conditions is very important in preparing the Fe−Ni−Cr coatings. The effects of PC electrodeposition parameters on the structural properties and corrosion resistance of Fe−Ni−Cr coatings have been reported in the above mentioned references. But, up to our knowledge, none of these studies has discussed the magnetic behaviors and tribological properties of Fe−Ni−Cr ternary coatings under different pulse current densities. In this study, Cr was added as the third element to Fe−Ni coatings and these deposits were prepared from a chloride bath. Also, the effects of applied current density on the surface morphologies, chemical compositions, magnetic behaviors, hardness and wear properties of the coatings were studied in details.

2 Experimental

The Fe−Ni−Cr coatings were produced by PC electrodeposition method from a chloride bath. Copper samples (10 mm × 10 mm × 1 mm) were used as cathodes and a sheet of 430 stainless steel (20 mm × 20 mm × 1 mm) was used as the anode. The surface of the copper substrates was polished mechanically with abrasive papers from 800 up to 3000 grade, and sequentially ultrasonically cleaned in acetone for 10 min. Then, these samples were cleaned with distilled water to remove contamination from the surface and then immersed immediately in the plating bath to allow the co-deposition of the Fe−Ni−Cr alloy coatings. These samples were fixed to be parallel to the anode at a distance of 3 cm from its surface. The purity of Cu cathodes was 99.98 wt.% and the chemical composition of 430 stainless steel anode is shown in Table 1. Moreover, the concentrations of the optimized chloride bath and the operating parameters of PC electro-deposition process are shown in Tables 2 and 3, respectively. The electrolyte was prepared by dissolving reagents in distilled water and the experiments were performed in a 100 mL plating cell. Direct current was supplied by using a digital coulometer (BHP 2056) without agitation and was converted to pulse current by a digital transformer.

The pH value of baths was maintained at 1.2−1.6 and controlled by using hydrochloric acid (HCl) and

Table 1 Chemical composition of 430 stainless steel anode

Element	Content/wt.%
Cr	≤0.12
Mn	1
Si	1
P	≤0.04
S	≤0.03
Cr	16−18
Ni	≤0.50

Table 2 Concentrations of optimized chloride bath for electro-deposition of Fe−Ni−Cr coatings

Bath composition	Concentration/(g·L^{-1})
Chromium chloride (CrCl$_3$·6H$_2$O)	200
Nickel chloride (NiCl$_2$·6H$_2$O)	50
Ferro chloride (FeCl$_2$·4H$_2$O)	20
Boric acid (H$_3$BO$_3$)	35
Ammonium chloride (NH$_4$Cl)	65
Sodium citrate dehydrate (Na$_3$C$_6$H$_5$O$_7$·2H$_2$O)	75
L-ascorbic acid (C$_6$H$_8$O$_6$)	3.5

Table 3 PC electrodeposition parameters for electrodeposition of Fe−Ni−Cr coatings

Electrodeposition parameter	Value
Current density/(mA·cm^{-2})	10, 20, 30, 40, 50
Duty cycle/%	50
Pulse frequency/Hz	100
Pulse on−off time/ms	5
Stirring speed/(r·min^{-1})	300
pH	1.2−1.6
Temperature/°C	40

sodium hydroxide (NaOH). Moreover, the ascorbic acid (AA) was used as an antioxidant in the bath to avoid anodic oxidation of Fe^{2+} to Fe^{3+} [14]. The coatings were fabricated at a constant temperature of 40 °C and the solution was stirred during plating by magnetic stirring at a speed of 300 r/min. The electric charge for plating the samples was kept constant at 50 C, which leads to the same coating thickness in each electrolyte. The duty cycle and the pulse frequency were at constant values of 50% and 100 Hz, respectively. While, the pulse current densities were varied at five different levels, i.e. 10, 20, 30, 40 and 50 mA/cm^2, and also, the corresponding deposition time was calculated from the Faraday's law [14].

The surface morphology and chemical composition of coatings were characterized by a scanning electron microscopy (SEM model WEGA/TESCAN) equipped with an energy dispersive X-ray (EDX) analyzer. The reported mass fraction of each element was the average of the three measurements at different locations for each sample. The structural analysis and grain size determination of coatings were investigated by X-ray diffraction (XRD) technique using Cu K$_\alpha$ radiation (BRUKER/D8 ADVANCED diffractometer, 30 kV and 30 mA). The results were interpreted by X-pert high score software, and the grains size (d) were determined by using Scherrer equation [14]:

$$d=0.9\lambda/(\beta\cos\theta) \tag{3}$$

where λ, β and θ are the wavelength of copper ($\lambda=$ 1.5406 Å), the full width at half-maximum (FWHM) of the peak and the diffraction angle, respectively. The scan was performed from 2θ angles of 30°−90° with a step size of about 0.03°. Moreover, magnetic properties of coatings were measured by a vibrating sample magnetometer (VSM) (Lakeshor 7404, Co., USA), and a parallel magnetic field of about ±2 MA/m was applied on the surface of each specimen. The dimensions of samples were 0.5 mm × 0.5 mm with 1 μm in thickness, and the magnetic measurements were done at room temperature. For magnetic measurements, the coating did not peel off from the copper substrate, and also a thin substrate was chosen to let the parallel magnetic field cross it easily. The hardness of samples was examined by using Vickers microhardness instrument, and a constant load of about 50 g was applied for 15 s. Measurements were taken at least 5 times for each coating and the corresponding average values were reported. Due to low penetration depth of the indenter, the copper substrate did not have any effect on the hardness measurement value. Furthermore, the wear resistance of coatings was evaluated by a pin-on-disk type wear testing instrument. The electroplated samples were under a load of 3 N, a rotation speed of 5 cm/s, a movement radius of 5 mm, and a sliding distance of 250 m. In this test, a pin of SAE 52100 hardened steel with a tip radius of 5 mm, a hardness of HV 800, a height of 50 mm and a surface roughness of 0.01 μm was used. The wear rate values of coatings were determined by the mass loss method using a digital microbalance (AND-GR202) with an accuracy of ±0.1 mg. Moreover, the worn surfaces and the type of wear mechanism were examined through SEM images.

3 Results and discussion

3.1 Morphology and composition of coatings

The effect of current density on surface morphology of the coatings is illustrated in Fig. 1. It is clear that the coatings prepared at lower current densities are uniform, very dense, smooth and almost without any micro-cracks. Such a homogeneous and dense structure can be explained due to the use of PC electrodeposition technique. In fact, the characteristics of this method reduce the growth of grains and earlier nuclei. Therefore, this effect creates the very dense and fine-grained structures in the deposited coatings [4,5,7,17,20]. However, by increasing the current density to 40 and 50 mA/cm^2, the surface morphology of the coatings showed a mixed structures of large nodules and rough cauliflowers (Figs. 1(d) and (e)). The main reason for the formation of this rough morphology can be related to higher co-deposition rate of Cr compared with deposition
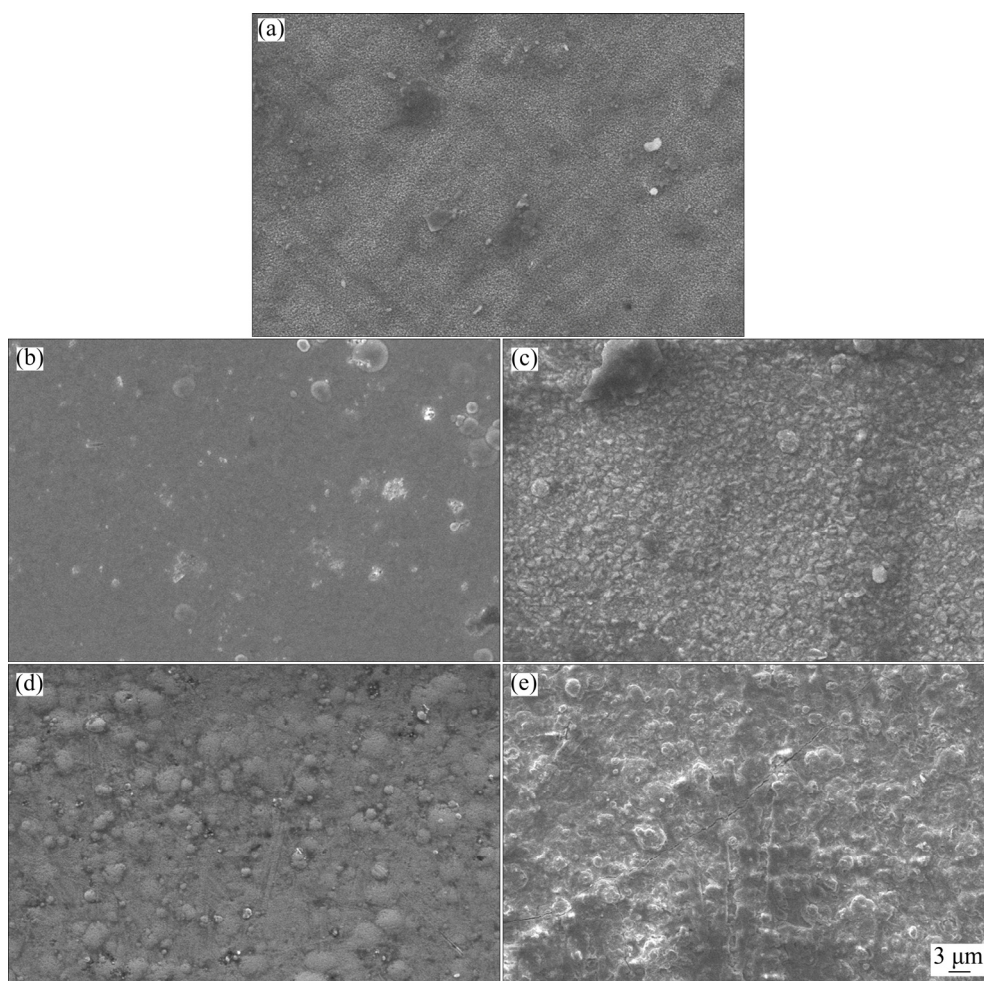
Fig. 1 SEM images of Fe−Ni−Cr alloy coatings prepared at different current densities: (a) 10 mA/cm^2; (b) 20 mA/cm^2; (c) 30 mA/cm^2; (d) 40 mA/cm^2; (e) 50 mA/cm^2

rates of Fe and Ni at higher current densities. Previous studies have reported that the surface morphology of coatings highly depends on the electrodeposition process conditions. It is observed that by increasing the current density, the surface of coatings became non-uniform and rough, and also, a few numbers of micro-cracks were formed on the surface [7,10,23−25]. The crystallization process occurred either by the build-up of old crystals, or with the formation and growth of new ones. These two factors are in competition with each other, and can be greatly influenced by different parameters. Low surface diffusion rates, high density of atoms, and high overpotentials are the effective parameters on the production of new nuclei [3,14,26].

Moreover, Fig. 1(e) shows a few numbers of micro-cracks on the surface of this sample. This behavior might be due to higher content of Cr in this coating, which was prepared at a current density of 50 mA/cm^2. In fact, cracking is a major problem in electrodepositing process of the Cr-based alloy coatings [4−7,17]. It is observed that the micro-cracks in Cr-based alloy coatings are due

to the decomposition of Cr hydrides and deposition stresses [5,7,10,25]. Based on previous studies, it is confirmed that the micro-cracks (the crack with micrometer width size) in Fe−Ni−Cr coatings could act as corrosive ways, because the substrate had been directly exposed to a corrosive medium. While, the Fe−Ni−Cr coatings with fine and thin cracks (smaller cracks with respect to micro-cracks) have a relatively high corrosion resistance [5,10,17,25].

However, the Fe−Ni−Cr coatings were prepared with less micro-cracks and just a few numbers of small and thin micro-cracks were obtained at a current density of 50 mA/cm^2. This unique behavior may be attributed to the use of pulse current in electrodeposition process. The results of previous studies indicated that the cracks on the surface of Fe−Ni−Cr coatings prepared by PC electrodeposition method are much less than those of the coatings produced by DC electrodeposition process [4−7,17]. In fact, PC electrodeposition provides the enough time for the abandoned hydrogen to exit from the surface of deposits. This liberation of hydrogen

during off time in PC electrodeposition method reduces the cracking effect of chromium and produce crack-free coatings [5,7,17]. Therefore, PC electrodeposition technique can lead to less micro-cracking and consequently improving the mechanical properties and corrosion resistance of the Cr-containing coatings [4,5,7,17]. Moreover, the coatings that were prepared at lower current densities had uniform surface morphology and smooth, metallic with fine grain structures.

Figure 2 shows chemical composition of the coatings produced at different current densities. It can be seen that the Fe, Ni and Cr contents of the coatings exhibit a strong dependence on the pulse current density. By increasing the current density from 10 to 50 mA/cm^2, the Fe and Ni contents were decreased from 73.05 wt.% and 26.20 wt.% to 69.85 wt.% and 24.29 wt.%, respectively. While, the Cr content of coatings was increased from 0.75 wt.% to 5.86 wt.%. On the other hand, at a constant current density, the Cr content in coatings was always less than that of Fe. Furthermore, the EDX results show that the decrease of Fe content was higher than that of Ni content by increasing the current density.
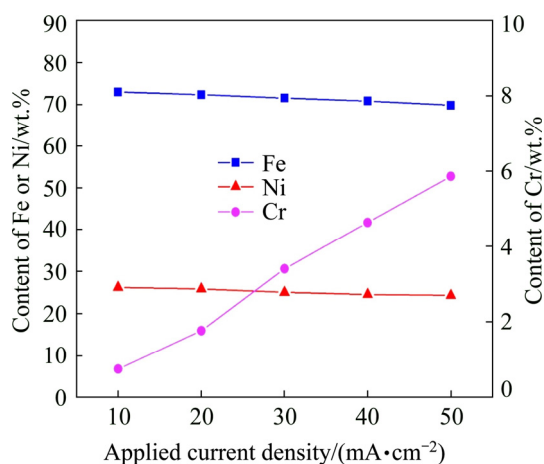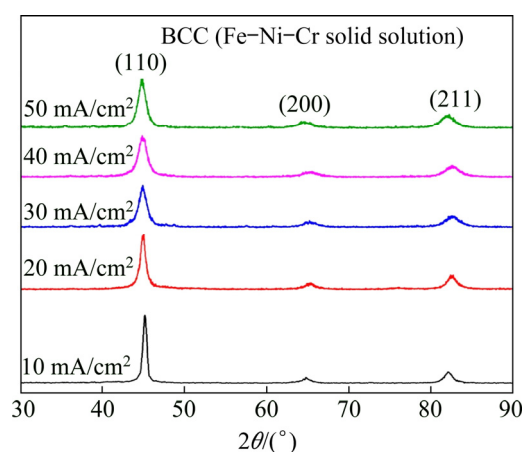

Fig. 2 Chemical compositions of coatings prepared at different current densities

The composition, microstructure and co-deposition rate of elements in the coatings depend considerably on the applied current density [1,6,7,12−14]. In fact, a reverse trend in the Cr content with increasing current density is due to the thermodynamic characteristics of Cr^{3+} reduction in the electrodeposition process of Fe−Ni−Cr ternary coatings [7,9,10,13]. To explain these behaviors, the mechanisms of co-deposition process of Fe, Ni and Cr during electrodeposition should be considered. From thermodynamic standpoint, the reduction potential of Cr^{3+} is more negative (lower) than that of Fe^{2+} and Ni^{2+}. Thus, the Cr deposition happened at higher deposition overpotentials (more negative potentials) compared with Fe and Ni

deposition [6,10,12,21]. At higher current densities, the reduction process of Fe^{2+} and Ni^{2+} species prevailingly happened under diffusion control. Therefore, by increasing the current density, the condition is superior for the increase in Cr content, and the Fe and Ni contents attain the minimum amounts in Fe−Ni−Cr coating systems [6,7,9]. Therefore, the use of higher current densities and increasing the concentration of Cr^{3+} in the baths are suitable for dominating the deposition rate of Cr over the co-deposition process of Fe and Ni, and also preparing the Fe−Ni−Cr coatings with higher Cr content [7,9,21,27]. Based on the results of electrodeposition, a single environmental friendly plating bath containing Fe^{2+}, Ni^{2+} and Cr^{3+} could produce Fe-based coatings with different concentrations of Cr.

3.2 Structural characterization

XRD studies were carried out to determine the crystal structure and grain size of electrodeposited coatings. The coating phases at various current densities were obtained from the peak profiles of the X-ray reflection plotted as a function of 2θ, as shown in Fig. 3. Comparing the XRD patterns of the samples with the standard JCPDS data showed that they have BCC crystal structure. Moreover, XRD measurement confirmed that the diffracted peaks are (110), (200) and (211) forms for all the produced coatings [10,27,28].

Fig. 3 XRD patterns of coatings obtained at different current densities

On the other hand, the chemical compositions of coatings in Fig. 2 show the presence of Ni and Cr in all coatings. However, careful observation of the XRD pattern shows only Fe peaks at all current densities. This indicates the complete dissolution of Ni and Cr in the iron matrix, and a single phase solid solution (consisting of crystalline Fe−Ni−Cr solid solution) is formed [10,27,28]. Moreover, the electrodeposition method is a non-equilibrium technique and the formed structures by this process are farer than those in

equilibrium phase diagram [27]. In fact, the structure of Fe−Ni−Cr coatings depends on the applied current density. At different current densities, the contents of Fe, Ni and Cr are changed, and this behavior leads to the formation of different crystalline peaks with high intensities [5,10,27,28].

Also, the fact that the peak shifts with increasing current density may be due to heterogeneous strain in the structure. Moreover, the Scherrer equation was used to study the influence of different current densities on the grain size, and (110) peaks were chosen for the grain size measurement of the coatings and the results are shown in Table 4. By increasing the current density, widening of the crystalline Fe peaks by significant decrease in their intensities confirms the grain size refinement in all coatings. Therefore, the average grain size of coatings was in the nano-metric range from 38 to 64 nm.

Table 4 Grain sizes of coatings at different applied current densities
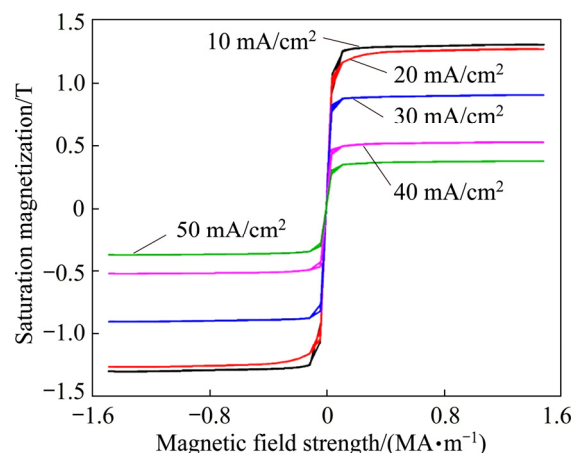
Sample No.	Current density/(mA·cm^{-2})	Grain size/nm
1	10	64
2	20	57
3	30	46
4	40	42
5	50	38

The rates of nucleation and grain growth are competing with each other and the difference between these factors determines the grain size of the coatings in this method. By increasing the current density in electrolyte, the nucleation rate overcomes the grain growth rate and this effect leads to a reduction in the average grains size of deposited alloys. In fact, increasing the overpotential leads to higher nucleation rates at higher current densities [14,23,29−31]. Eventually, as a result, with increasing the current density, the grains size has decreased [30−31]. Therefore, the current density is an important parameter in determining the grain size of Fe−Ni−Cr alloy deposits. The grain size of coatings becomes finer from 64 to 38 nm, by increasing the applied current density from 10 to 50 mA/cm^2 (Table 4).

3.3 Magnetic behaviors

The magnetic behavior was determined by measurement of saturation magnetization (M_s) and the coercivity (H_c) values [6,14,21,28]. While, the saturation magnetization is an intrinsic property and depends on the chemical composition of materials, whereas the coercivity is an extrinsic feature [6,14,24]. The hysteresis curves of the coatings prepared at different current densities are shown in Fig. 4. Furthermore, the changes

of saturation magnetization and coercivity values of the coatings as a function of current density are given in Table 5.

Fig. 4 Hysteresis loops of Fe−Ni−Cr coatings prepared at different current densities

Table 5 Saturation magnetization and coercivity values of Fe−Ni−Cr coatings as function of applied current density

Sample No.	Current density/ (mA·cm^{-2})	M_s/T	H_c/(A·m^{-1})
1	10	1.30	157.6
2	20	1.27	159.2
3	30	0.90	248.8
4	40	0.52	328.8
5	50	0.37	356.0

By increasing the current density, the saturation magnetization (M_s) and coercivity (H_c) values of coatings were decreased and increased, respectively. This behavior could be due to the chemical composition variations with current density. EDX results show that by linearly increasing the current density, the Fe and Ni contents were decreased, while the co-deposition rate of Cr was increased. Fe has the superior magnetic properties among the soft magnetic materials and its content is an effective parameter on the magnetic behaviors of the coatings. Moreover, Ni is also an important element with soft magnetic properties [3,6,14,21]. Therefore, a decrease in Fe and Ni amounts leads to a sharp decline of the saturation magnetization and an increase of the coercivity of the coatings [3,6,24,32]. Furthermore, the saturation magnetization value is inversely proportional to Cr content of the coatings. In fact, the higher content of Cr at high current densities leads to the decrease in the M_s values, because Cr is a non-magnetic element and has the paramagnetic behavior [33,34].

However, unlike the saturation magnetization, the coercivity depends on several factors such as the grain

size, microstructure and chemical composition. But, the grain size is the most important parameter, which can affect the coercive field of the coatings [3,14,24,35]. The previous studies indicated that the grain size reduction leads to an increase in the coercivity value [3,24,36−38]. While in a few researches, there are different viewpoints for the influence of grain size on the coercivity. It is reported that at grain size larger than that of the magnetic exchange length (L_{ex}), domain wall pining which is due to grain boundaries would occur. The authors in Refs. [15,35,38] presented the random anisotropy model (RAM) for nanostructured magnetic alloys. According to this theory, H_c depends on the grain size (D) and L_{ex} [14,39,40]. In fact, the grain size reduction leads to the decrease of the H_c when $D<L_{ex}$. When the grain size is smaller than L_{ex}, domain wall effect is crossed out, and each grain acts as a single domain. The previous studies reported that the L_{ex} of nanocrystalline Fe−Ni coatings was decreased by increasing the Fe amount [14,40]. As the grains size of the samples was larger than the exchange length for all the coatings ($D>L_{ex}$), according to the RAM theory, the grain size reduction leads to the increase of the H_c values. The variations of grain size and coercivity as a function of applied current density are shown in Fig. 5. As seen in Fig. 5, the grain size has a great influence on the H_c values. The results showed that by increasing the current density from 10 to 50 mA/cm², the grains size was decreased from 64 to 38 nm and the coercivity value was increased from 157.6 to 356.0 A/m. Moreover, H_c values of the coatings were increased, by increasing the amount of Cr in Fe−Ni matrix. The maximum value of coercivity was obtained for the sample with 5.75 wt.% Cr (356.0 A/m).
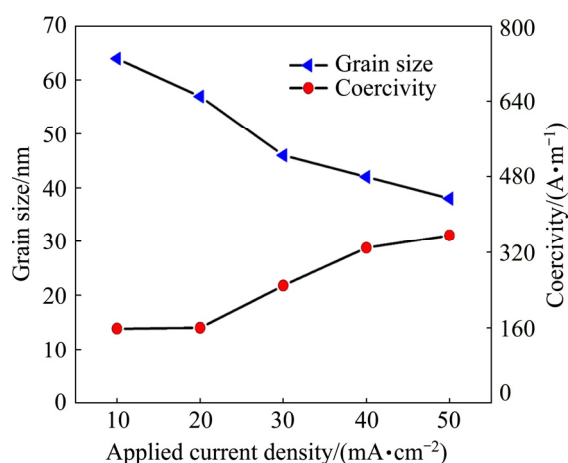
Fig. 5 Variations of grain size and coercivity as function of applied current density

VSM results revealed that the coercivity value shows a regular behavior with the Cr content [6,33,34]. Moreover, magnetic measurements showed that the hysteresis loops were weedy and narrow. This behavior suggested that the Fe−Ni−Cr coatings exhibit the soft magnetic property [24,28]. In this study, the highest saturation magnetization (1.30 T) and the lowest coercivity (157.6 A/m) values were obtained for the sample electroplated at a current density of 10 mA/cm². Generally, the VSM results revealed that there was a linearly relationship between the magnetization feature and the chemical composition of Fe−Ni−Cr coatings. The M_s values of these coatings were decreased, when the contents of Fe and Ni were decreased, and the Cr content was increased. The mechanical mixture of a ferro-magnetic material with a paramagnetic component leads to linear decrease of the M_s value [14,33,34]. On the other hand, the grain size reduction and higher Cr content lead to the increase in the coercive fields [24,33,34,37]. However, the H_c values were very low and less than 400 A/m. This behavior is due to the unique advantage of PC electrodeposition technique. The type of applied current in electrodeposition process is an effective parameter on the grain size refinement and afterwards the magnetic properties. In fact, decreasing the H_c value in the electroplated coatings by pulse current (PC) and pulse reverse current (PRC) electrodeposition is more than that of the coatings produced with direct current (DC) method because the grain size of coatings prepared by these two methods is less than that of DC method [6,14].

3.4 Microhardness measurements

The grain size and chemical composition of the deposited alloys are two effective factors on the hardness of coatings [6,13]. The microhardness variations of the coatings with applied current density are exhibited in Table 6. With regard to the experimental observation, the penetration depth is lower than the coating thickness and the measured hardness is related to the coating. Therefore, the penetration depth of the indenter is related to the hardness of the coating that is affected by chemical composition and grain size. As seen in Table 6, the sample prepared at a current density of 10 mA/cm² has the lowest microhardness value (HV 458). However, by increasing the current density from 10 to 50 mA/cm², the microhardness was increased to the maximum value (HV 583). The Fe and Ni contents were not identical at different current densities. The Fe and Ni are soft magnetic materials, and these elements have low hardness [3,6,26]. Therefore, by increasing the pulse current density, the hardness property was improved due to the reduction of Fe and Ni amounts in the coatings. Moreover, increasing the current density leads to enhancing the Cr content in Fe−Ni matrix. Cr, as hard element, affects the hardness and the alloy coatings with the higher Cr content have higher hardness. In fact, Cr plays an important role in improving the mechanical

properties of Fe−Ni-based alloys. These results are in agreement with those of other studies [7,13,41,42].

Table 6 Microhardness variations of coatings deposited at different applied current densities

| Sample No.	Applied current density/ $(mA \cdot cm^{-2})$	Microhardness $(HV_{0.05})$
1	10	458
2	20	486
3	30	532
4	40	557
5	50	583

On the other hand, the grain size is also an effective parameter on hardness of the nanocrystalline coatings. By increasing the current density, overpotential and the nucleation rate were increased. This behavior improves the hardness of the coatings due to modification of the growth and reduction of grain size [4,6,30,31,43]. This induces a significant increase in the mechanical properties of nanocrystalline alloys due to Hall−Petch theory [6,30,31,43]. The nucleation mechanism of small grains on the surface leads to the modification and refinement of the structure. In fact, the smaller grains impede for the dislocation motion in metallic matrix, and this effect improves the hardness of the coatings [14,41]. It is reported that by PC electrodeposition method the fine-grained structures and nanocrystalline coatings with higher hardness can be prepared [6,11,30,31]. The sample prepared at a current density of 50 mA/cm^2 with higher Cr content (5.86 wt.%) and smaller grain size (38 nm) shows the highest hardness among all the investigated coatings.

3.5 Tribological properties

The morphology, phase structure, micro-cracks and the external parameters of wear process (like load, distance and speed) are effective factors on improving the wear resistance. However, the chemical composition and hardness are the main important parameters that affect the friction coefficient and wear rate of the coatings [6,21,29]. The variations of friction coefficient and wear rate of Fe−Ni−Cr coatings as a function of applied current density are presented in Figs. 6(a) and (b), respectively.

As seen in Fig. 6, the friction coefficient and wear rate values of coatings were decreased with increasing the applied current density. The coefficient of friction is one of the effective parameters, which plays a critical role in the wear behavior of coatings [6,29,44]. It is obvious that the friction coefficient of coating prepared at a current density of 50 mA/cm^2 is much lower than that of sample prepared at a current density of

10 mA/cm^2. This behavior is due to variations of the composition and the grain size of coatings. Iron and nickel are much softer than chromium and the coefficient of friction is a function of softness of the material. In fact, the amounts of wear debris are more on the surface of soft materials. These wear debris act as the contact points between the surface and abrasive pin of coatings, and this leads to the increase in the friction coefficient value [14,43].
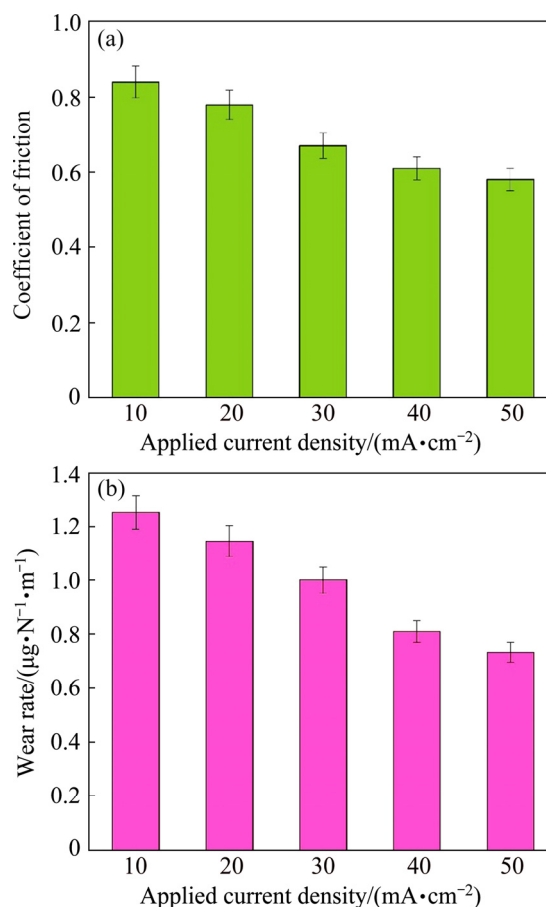
Fig. 6 Wear resistance measurements of alloy coatings as function of applied current density: (a) Coefficient of friction; (b) Wear rate

Also, employing the PC electrodeposition method caused to produce the fine and compact microstructures with good wear resistance [6,41]. Increasing the current density can improve the tendency towards forming more grains, and the number of crystal nuclei will increase. Therefore, the grains will be further refined and this issue will account for improving the mechanical properties of coatings [14]. On the other hand, the movement of dislocations was encountered with difficulty owing to pile-up of dislocations in the nanostructure materials. Thus, the grain size reduction led to lower friction coefficient and wear rate values, and also, exhibited an excellent tribological behavior in the alloy and composite coatings [14,41,45]. As seen in

Fig. 6(b), the applied current density had a positive effect on wear resistance, and the values of mass loss of coatings were gradually decreased at high current densities. The wear rate of prepared coating at a current density of 50 mA/cm^2 is lower than that of the sample prepared at a current density of 10 mA/cm^2. Therefore, the tribological properties of the coatings were improved by decreasing the Fe and Ni contents, grain size reduction and increasing the co-deposition rate of Cr in the Fe−Ni matrix which are favored by increasing the applied current density [14,44]. This implies that the electroplated coating at a current density of 50 mA/cm^2 exhibits the best wear resistance (Fig. 6(a)).

Archard wear equation revealed the relationship between the wear resistance and hardness of the coatings. In fact, Archard calculated the wear rate of the coatings by Eq. (4) [41,42]

$$\Delta V = \frac{KLS}{H} \qquad (4)$$

where ΔV is the wear volume, L is the normal load, S is the sliding distance for every cycle, H is the micro-hardness, and K is the coefficient of wear loss [41,42]. In this study, K, L and S factors are constant values for all of the experiments. Therefore, there is a linear relationship between ΔV and $1/H$. The effect of microhardness on the friction coefficient and mass loss of the coatings is presented in Fig. 7. According to the Archard theory, better wear resistance and improvement of the tribological behavior of coatings can be attributed to their higher hardness [41,42,46].
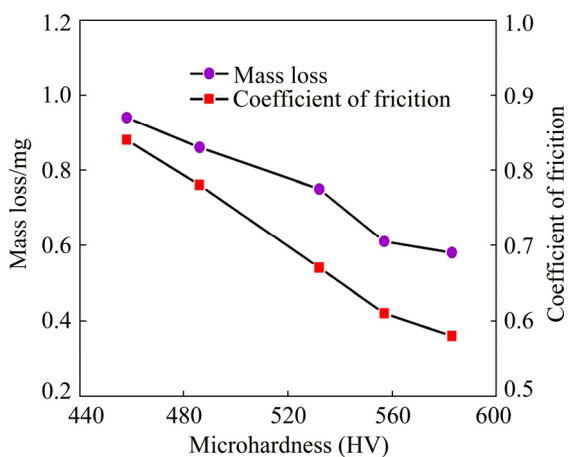

Fig. 7 Effect of microhardness on friction coefficient and mass loss of Fe−Ni−Cr alloy coatings

By increasing hardness, real contact area between the abrasive pin and the surface of samples was decreased. This effect led to the decrease in the friction coefficient and wear rate [41,44,46]. Generally, based on these reasons, the hardness property was believed to be the dominating factor for reducing the friction coefficient

and wear rate values. Moreover, we can produce the Fe−Ni magnetic coatings with superior mechanical properties and unique magnetic behavior by using the PC electrodeposition method.

SEM micrographs of the worn surfaces of coatings are illustrated in Fig. 8. As seen in Figs. 8(a) and (b), the wear track of coating prepared at a current density of 10 mA/cm^2 is smoother, and also, the penetration of the abrasive pin inside this sample is deeper than that of the prepared sample at a current density of 50 mA/cm^2. Moreover, the plastic deformation and some deformed layers were observed on the wear surface of the first sample. This issue is due to the lower hardness and weaker wear resistance of the first sample compared with other two coatings prepared at higher current densities. In fact, the wear track depth and width have the inverse relationship with the wear resistance of the coatings [8,14,19,20]. Also, it is observed that the compressed laminates in the zones similar to islands with an intense adhesion along the sliding direction on the surface of prepared sample at a current density of 10 mA/cm^2 are formed. This behavior suggested that the dominant wear mechanism for this coating was adhesive-type one due to the nature of the soft magnetic materials [14,20,47].

The Fe−Ni-based coatings have low hardness and wear resistance. Also, in these coatings the presence of adhesive mechanism leads to the increase in the friction coefficient and mass loss values [4,8,14,47]. It is reported that the adhesive wear mechanism is associated with both compaction and shear mechanisms. This behavior leads to the plastic deformation and transfers the wear debris on the worn surface of coatings. The presence of these wear debris can increase the friction coefficient and wear rate values of the coatings because the removed wear debris from Fe−Ni−Cr coatings mainly act as abrasive agents [14,19,20,47]. The deep abrasive grooves and wear debris were observed on the worn surface of the prepared sample at a current density of 10 mA/cm^2. While the comparison of the worn surfaces of this sample with those of other coatings shows that the abrasive grooves and the amount of wear debris were significantly decreased by increasing the applied current densities (Figs. 8(c−f)). This indicates the change of wear mechanism from the adhesive type to the abrasive one. These results can be attributed to the wear theories because of a wear mechanism transition related to the surface properties of the worn materials. In fact, the presence of Cr during the wear track determines the abrasive wear regime. The addition of Cr into the soft magnetic materials (like Fe−Ni matrix) can largely decrease the friction coefficient and wear rate values which improve the wear resistance of the coatings [14,41,42].
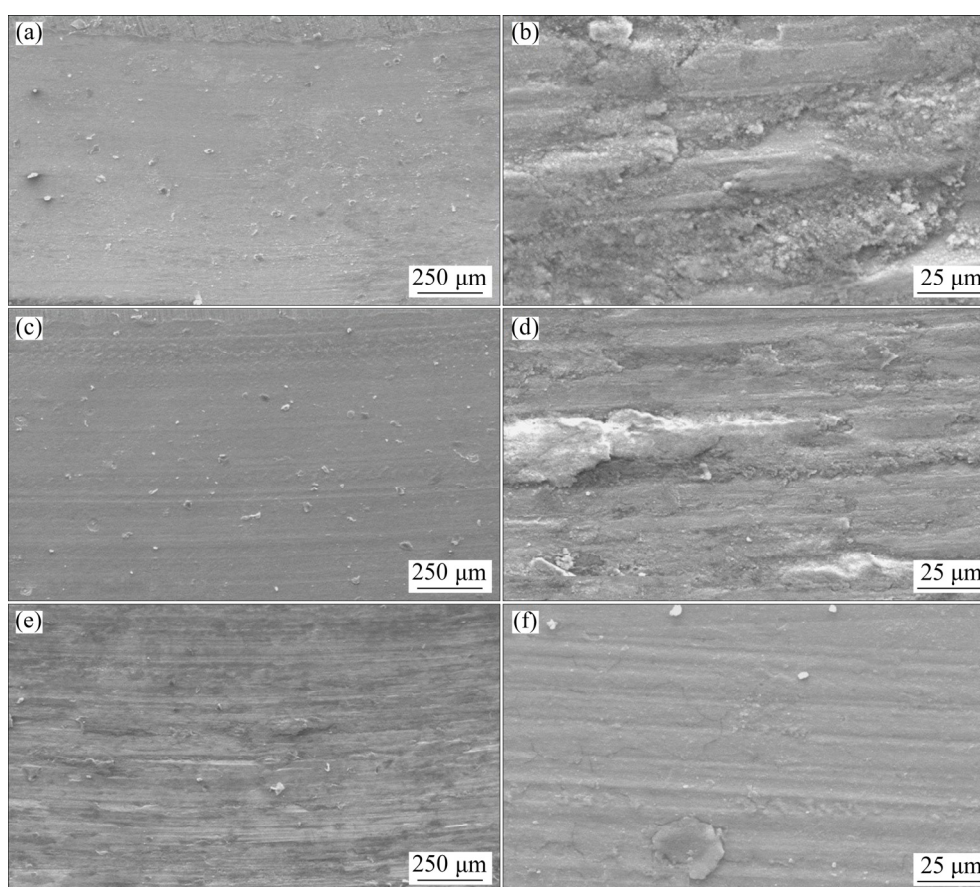
Fig. 8 SEM micrographs of worn surfaces of coatings deposited at different current densities under low and high magnifications: (a, b) 10 mA/cm^2; (c, d) 30 mA/cm^2; (e, f) 50 mA/cm^2

On the worn surface of sample prepared at a current density of 50 mA/cm^2, the appearance of the wear scar was not smooth. Moreover, it can be seen that the abrasive continuous scratches were parallel to the sliding direction on the worn surface of this sample. These features were created on the surface of the sample with abrasive wear mechanism (Figs. 8(e) and (f)). During the wear process of the coatings with abrasive mechanism, wear debris and particles were displaced on either side of the abrasion groove [8,14]. Co-deposition of Cr inside the Fe−Ni matrix led to the increase in the hardness value and therefore reduction of plastic deformation on the worn surface of the coatings (Figs. 8(c−f)). The presence of Cr also led to the increase in the anti-scratching abilities and the decrease in the width of the wear track, thereby these issues improve the tribological behavior of the coatings [4,20].

Furthermore, the grooves depth, fallen-off parts and delamination were clearly observed on the worn surface of the prepared sample at a current density of 10 mA/cm^2. For coating produced at a current density of 50 mA/cm^2, these grooves and defects were almost shallow and unnoticeable. Also, this sample had a narrower and smoother wear track compared with other specimens.

This behavior was in agreement with the results of microhardness and wear rate of electrodeposited coatings. This indicated that the prepared coatings at higher current densities had much better wear resistance. Moreover, during the sliding, the mass amount of the wear debris on the surface of coating prepared at a current density of 50 mA/cm^2 (with 5.86 wt.% Cr and grain size of 38 nm) was less than that of the sample produced at a current density of 10 mA/cm^2 (with 0.75 wt.% Cr and grain size of 64 nm). Furthermore, the investigation of the worn surfaces indicated that the dominant wear mechanism for specimen prepared at a current density of 10 mA/cm^2 was adhesive type one. By increasing the current density and Cr content, the hardness and resistance to the surface micro-cutting of coatings were increased. These effects led to the shift in the wear mechanism to abrasive type and finally, a mixed mechanism of adhesive and abrasive on the worn surfaces of the coatings produced at 30 and 50 mA/cm^2 current densities was observed.

In fact, the observations of worn surfaces showed that the presence of Cr created the plastically deformed edges on the surface of coatings. This behavior suggested that the adhesive and abrasive type regimes were the

main wear mechanisms in Fe−Ni−Cr coatings. Generally, the results of tribological behavior showed that the smaller grain size, lower Fe and Ni contents, higher co-deposition rate of Cr in Fe−Ni matrix, and also, using the PC electrodeposition method help for the increase of the hardness, and the reduction of the friction coefficient and wear rate values. These effects significantly improved the wear resistance and better mechanical properties [14,41,42,44].

4 Conclusions

(1) The produced nanocrystalline Fi−Ni−Cr coatings were uniform with mixture of fine nodules and cauliflower morphologies at low current densities. While by increasing the current density, the alloy coatings showed the non-uniform and rough cauliflower morphologies with a few micro-cracks on the surfaces.

(2) At higher current densities, Cr content was increased at expense of Fe and Ni amounts in the alloy coatings due to the creation of higher overpotential.

(3) X-ray diffraction patterns showed that the single-phase solid solutions (consisting of crystalline Fe−Ni−Cr phase) were formed with BCC crystal structure, which is confirmed by the formation of the (110), (200) and (211) peaks at various current densities. Furthermore, the increase of current density led to the domination of nucleation rate over the grain growth one which has a positive effect on the grain size refinement.

(4) Increasing the current density led to the decrease in the saturation magnetization and the increase in the coercivity by the smaller grain size and higher co-deposition rate of Cr in the coatings. The lowest saturation magnetization (0.37 T) and highest coercivity (356.0 A/m) were obtained for the sample electroplated at a current density of 50 mA/cm^2.

(5) By decreasing the Fe and Ni amounts, grain size, and increasing the Cr content, the wear resistance and hardness properties of these coatings were improved. The highest friction coefficient and wear rate values were obtained for the coating electrodeposited at a current density of 10 mA/cm^2. Furthermore, the high amounts of wear debris at low current densities in resulted in the adhesive wear mechanism. However, the plastic deformed layers and the wear debris were decreased by increasing the current density and Cr content. These issues led to the observation of the adhesive and abrasive wear mechanisms on the worn surfaces of coatings.

Acknowledgements

References

[1] GHORBANI M, IRAJI ZAD A, DOLATI A, GHASEMPOUR R. The effect of the Cr and Mo on the physical properties of electrodeposited Ni−Fe alloy films [J]. Journal of Alloys and Compounds, 2005, 386: 43−46.

[2] ATAEE-ESFAHANI H, VAEZI M R, NIKZAD L, YAZDANI B, SADRNEZHAAD S K. Influence of SiC nanoparticles and saccharin on the structure and properties of electrodeposited Ni−Fe/SiC nanocomposite coatings [J]. Journal of Alloys and Compounds, 2009, 484: 540−544.

[3] PAVITHRA G P, HEGDE A C. Magnetic property and corrosion resistance of electrodeposited nanocrystalline iron–nickel alloys [J]. Applied Surface Science, 2012, 258: 6884−6890.

[4] TORABINEJAD V, SABOUR ROUHAGHDAM A, ALIOFK-HAZRAEI M, ALLAHYARZADEH M H. Electrodeposition of Ni−Fe and Ni−Fe−(nano Al$_2$O$_3$) multilayer coatings [J]. Journal of Alloys and Compounds, 2016, 657: 526−536.

[5] TORABINEJAD V, ALIOFKHAZRAEI M, SABOUR ROUHAGHDAM A, ALLAHYARZADEH M H. Corrosion properties of Ni−Fe−Cr(III) multilayer coating synthesized via pulse duty cycle variation [J]. Materials and Corrosion, 2017, 68: 347−354.

[6] TORABINEJAD V, ALIOFKHAZRAEI M, ASSAREH S, ALLAHYARZADEH M H, SABOUR ROUHAGHDAM A. Electrodeposition of Ni−Fe alloys, composites, and nano coatings: A review [J]. Journal of Alloys and Compounds, 2017, 691: 841−859.

[7] ADELKHANI H, ARSHADI M R. Properties of Fe−Ni−Cr alloy coatings by using direct and pulse current electrodeposition [J]. Journal of Alloys and Compounds, 2009, 476: 234−237.

[8] TORABINEJAD V, ALIOFKHAZRAEI M, SABOUR ROUHA-GHDAM A, ALLAHYARZADEH M H. Tribological properties of Ni−Fe−Co multilayer coatings fabricated by pulse electrodeposition [J]. Tribology International, 2009, 106: 34−40.

[9] QI J Z, LI B Y, YI X, JIAN F G, QING D Z, JI B J, QIONG Y Z. The electrodeposition of Ni−Fe−Cr alloy coatings on mild steel surfaces and evaluation of corrosion resistance. [J]. Advanced Materials Research, 2013, 948: 785−786.

[10] CHING A H, JO H C, CHAO Y C, KANG Y L, MAYER J. Microstructure and electrochemical corrosion behavior of Cr−Ni−Fe alloy deposits electroplated in the presence of trivalent Cr ions [J]. Thin Solid Films, 2013, 544: 69−73.

[11] HE X K, HOU B L, CAI Y X, LI C, JIANG Y M, WU L Y. Electrodepositing behaviors and properties of nano Fe−Ni−Cr/SiC composite coatings from trivalent chromium baths containing compound carboxylate−urea system [J]. Journal of Nanoscience and Nanotechnology, 2013, 13: 4031−4039.

[12] XU L J. Preparation and characterization of nanocrystalline Fe−Ni−Cr alloy electrodeposits on Fe substrate [J]. Journal of applied electrochemistry, 2009, 39: 713−718.

[13] KANG J C, LALVANI S B, MELENDRES C A. Electrodeposition and characterization of amorphous Fe−Ni−Cr-based alloys [J]. Journal of Applied Electrochemistry, 1995, 25: 376−383.

[14] YOUSEFI E, SHARAFI S, IRANNEJAD A. The structural, magnetic, and tribological properties of nanocrystalline Fe−Ni permalloy and Fe−Ni−TiO$_2$ composite coatings produced by pulse electro co-deposition [J]. Journal of Alloys and Compounds, 2018, 753: 308−319.

[15] SARAVANAN G, MOHAN S. Electrodeposition of Fe−Ni−Cr alloy from deep eutectic system containing choline chloride and ethylene glycol [J]. International Journal Electrochemical Science, 2011, 6: 1468−1478.

[16] ZENG Z X, ZHANG Y X, ZHAO W J, ZHANG J Y. Role of complexing ligands in trivalent chromium electrodeposition [J]. Surface and Coating Technology, 2011, 205: 4771−4775.

[17] DENG S H, GONG Z Q. The electrochemical behaviour of pulse-plated nanocrystalline iron−nickel−chromium alloy [J]. Anti-Corrosion Methods and Materials, 2003, 50: 267−270.

[18] CHING A H, CHAO Y C, MAYER J, WEIRICH T, ISKANDAR R. Nanosegregation of ternary Cr−Ni−Fe alloy deposits electrodeposited from a Cr^{3+}-based bath [J]. Materials Letters, 2013, 93: 107−110.

[19] KARTALA M, UYSAL M, GUL H, ALP A, AKBULUT H. Effect of surfactant concentration in the electrolyte on the tribological properties of nickel−tungsten carbide composite coatings produced by pulse electro co-deposition [J]. Applied Surface Science, 2015, 345: 328−336.

[20] PARIDA G, CHAIRA D, KUMAR CHOPKAR M, BASU A. Synthesis and characterization of Ni−TiO_2 composite coatings by electro-co-deposition [J]. Surface and Coating Technology, 2011, 205: 4871−4879.

[21] DOLATI A, GHORBANI M, AFSHAR A. The electrodeposition of quaternary Fe–Cr–Ni–Mo alloys from the chloride-complexing agent electrolyte [J]. Surface and Coating Technology, 2003, 166: 105–110.

[22] WANG L P, GAO Y, XU T, XUE Q J. Corrosion resistance and lubricated sliding wear behaviour of novel Ni–P graded alloys as an alternative to hard Cr deposits [J]. Applied Surface Science, 2006, 252: 7361–7372.

[23] LAJEVARDI S A, SHAHRABI T. Effects of pulse electrodeposition parameters on the properties of Ni–TiO_2 nanocomposite coatings [J]. Applied Surface Science, 2010, 256: 6775–6781.

[24] GHAFERI Z, SHARAFI S, BAHROLOLOOM M E. Effect of current density and bath composition on crystalline structure and magnetic properties of electrodeposited FeCoW alloy [J]. Applied Surface Science, 2015, 355: 766–773.

[25] CHING A H, CHE K L, CHAO Y C. Hardness variation and corrosion behavior of as-plated and annealed Cr–Ni alloy deposits electroplated in a trivalent chromium-based bath [J]. Surface and Coating Technology, 2009, 203: 3686–3691.

[26] EBRAHIMI F, LI H Q. Structure and properties of electrodeposited nanocrystalline FCC Ni−Fe alloy [J]. Reviews on Advanced Materials Science, 2003, 5: 134−138.

[27] TAVOOSI M, BARAHIMI A. Corrosion behavior of amorphous–nanocrystalline Fe−Ni−Cr electrodeposited coatings Plating [J]. Surfaces and Interfaces, 2017, 8: 103−111.

[28] KANAGARAJ R, KANNAN R, GANESAN S. Synthesis and characterization of electrodeposited NiFeCr thin films [J]. Journal of Ovonic Research, 2014, 10: 197−204.

[29] KUNG H H, YANN C C. Preparation and wear resistance of pulse electrodeposited Ni−W/Al_2O_3 composite coatings [J]. Applied Surface Science, 2011, 257: 6340−6346.

[30] LI Y D, JIANG H, HUANG W H, TIAN H. Effects of peak current density on the mechanical properties of nanocrystalline Ni–Co alloys produced by pulse electrodeposition [J]. Applied Surface Science, 2008, 254: 6865−6869.

[31] TURY B, LAKATOS-VARSÁNYI M, ROY S. Ni–Co alloys plated by pulse currents bath [J]. Surface and Coating Technology, 2006, 200: 6713−6717.

[32] KOO B K, YOO B Y. Electrodeposition of low-stress NiFe thin films from a highly acidic electrolyte [J]. Surface and Coating Technology, 2010, 205: 740−744.

[33] KARIMI S, KAMELI P, AHMADVAND H, SALAMATI H. Effects of Zn−Cr substitution on the structural and magnetic properties of $Ni_{1−x}Zn_xFe_{2−x}Cr_xO_4$ ferrites [J]. Ceramics International, 2016, 42: 16948−16955.

[34] AUBRY E, LIU T, BILLARD A, DEKENS A, PERRY F, STEPHANCE M, TAMOS H. Influence of the Cr and Ni concentration in CoCr and CoNi alloys on the structural and magnetic properties [J]. Journal of Magnetism and Magnetic Materials, 2017, 422: 391−396.

[35] GHAFERI Z, SHARAFI S, BAHROLOLOOM M E. The role of electrolyte pH on phase evolution and magnetic properties of CoFeW codeposited films [J]. Applied Surface Science, 2016, 375: 35−41.

[36] MEHRIZI S, HEYDARZADEH SOHI M, SEYYED EBRAHIMI S A. Study of microstructure and magnetic properties of electrodeposited nanocrystalline CoFeNiCu thin films [J]. Surface and Coating Technology, 2011, 205: 4757−4763.

[37] KOCKAR H, OZERGIN E, KARAAGAC O, ALPER M. Characterisations of CoFeCu films: Influence of Fe concentration [J]. Journal of Alloys and Compounds, 2014, 586: 326−330.

[38] BAHRAMI A H, SHARAFI S, AHMADIAN BAGHBADERANI H. The effect of Si addition on the microstructure and magnetic properties of permalloy prepared by mechanical alloying method [J]. Advanced Powder Technology, 2013, 24: 235−241.

[39] KHAZAEI FEIZABAD M H, SHARAFI S, KHAYATI G R, RANJBAR M. Effect of process control gent on the structural and magnetic properties of nano/amorphous $Fe_{0.7}Nb_{0.1}Zr_{0.1}Ti_{0.1}$ powders prepared by high energy ball milling [J]. Journal of Magnetism and Magnetic Materials, 2018, 449: 297−303.

[40] JING P P, LIU M T, PU Y P, CUI Y F, WANG Z, WANG J B, LIU Q F. Dependence of phase configurations, microstructures and magnetic properties of iron–nickel (Fe−Ni) alloy nanoribbons on deoxidization temperature in hydrogen [J]. Scientific Reports, 2016, 6: 1010−1038.

[41] ZHOU Y B, ZHAO G G, ZHANG H J. Fabrication and wear properties of co-deposited Ni−Cr nanocomposite coatings [J]. Transactions of Nonferrous Metals Society of China, 2010, 20: 104−109.

[42] SHEIBANI AGHDAM A, ALLAHKARAM S R, MAHDAVI S. Corrosion and tribological behavior of Ni−Cr alloy coatings electrodeposited on low carbon steel in Cr(III)−Ni(II) bath [J]. Surface and Coating Technology, 2015, 281: 144−149.

[43] PWASEKAR N, HARIDOSS P, SESHADRI S K, SUNDARARAJAN G. Sliding wear behavior of nanocrystalline nickel coatings: Influence of grain size [J]. Wear, 2012, 296: 536−546.

[44] PRIYAN S, AZAD A, ARAFFATH Y. Influence of HVOF parameters on the wear resistance of Cr_3C_2−NiCr coating [J]. Journal of Materials Science and Surface Engineering, 2016, 4: 355−359.

[45] ÖZKAN S, HAPÇI G, ORHAN G, KAZMANLI K. Electrodeposited Ni/SiC nanocomposite coatings and evaluation of wear and corrosion properties [J]. Surface and Coating Technology, 2013, 232: 734−741.

[46] XIE X L, LEI Z, XIAO J K, QIAN Z Y, TAO Z, ZHOU K C. Sliding electrical contact behavior of AuAgCu brush on Au plating [J]. Transactions of Nonferrous Metals Society of China, 2015, 25: 3029−3036.

[47] CHEN L, WANG L P, ZENG Z X, ZHANG J Y. Effect of surfactant on the electrodeposition and wear resistance of Ni–Al_2O_3 composite coatings [J]. Materials Science and Engineering A, 2006, 434: 319−325.

脉冲电流法制备纳米晶 Fe–Ni–Cr 合金涂层的电沉积及表征

Ebrahim YOUSEFI[1,2], Ahmad IRANNEJAD[1,3], Shahriar SHARAFI[1,3]

1. Department of Nano technology, Mineral Industries Research Center,
Shahid Bahonar University of Kerman, Kerman 7618868366, Iran;

2. Young Researchers Society, Shahid Bahonar University of Kerman, Kerman 7618868366, Iran;

3. Department of Material Science and Engineering, Shahid Bahonar University of Kerman, Kerman 7618868366, Iran

摘　要：采用脉冲电流技术电沉积纳米晶 Fe–Ni–Cr 涂层。SEM 测试结果表明，在低电流密度下，涂层为小结节和细小菜花结构的混合形态；而在高电流密度下，Cr 含量随着涂层中 Fe 和 Ni 含量的降低而增加。XRD 谱证实，脉冲电流密度对晶粒细化具有积极作用。振动样品磁强计(VSM)测量结果表明，随着电流密度的提高，由于 Cr 含量的增加和晶粒尺寸的减小，饱和磁化强度降低、矫顽力增大。通过提高脉冲电流密度，可以降低摩擦因数和磨损率。此外，在磨损表面观察到粘着和磨粒磨损机制。随着脉冲电流密度提高，犁沟和磨屑的数量减少。

关键词：脉冲电沉积；电流密度；纳米晶 Fe–Ni–Cr 合金涂层；磁学行为；摩擦学性能

(Edited by Wei-ping CHEN)